СВЕРХБЫСТРАЯ ЭЛЕКТРОННАЯ КРИСТАЛЛОГРАФИЯ И НАНОКРИСТАЛЛОГРАФИЯ: ДЛЯ ХИМИИ, БИОЛОГИИ И НАУК О МАТЕРИАЛАХ. ЧАСТЬ I. СВЕРХБЫСТРАЯ ЭЛЕКТРОННАЯ КРИСТАЛЛОГРАФИЯ

Л. Шефер, Ю.И. Тарасов, А.В. Кошелев, А.А. Ищенко

Лотар Шефер

Кафедра химии и биохимии, Университет штата Арканзас, Фейетвилл, AR 72701, США
E-mail: schafer@uark.edu

Юрий Игоревич Тарасов

Кафедра физики и технической механики, Институт тонких химических технологий, Московский технологический университет, просп. Вернадского, 86, Москва, Российская Федерация, 119571
Объединенный институт высоких температур РАН, Москва, ул. Ижорская, 13, стр. 2, 125412
E-mail: y.i.tarasov@mitht.org

Александр Владимирович Кошелев

Кафедра аналитической химии, Институт тонких химических технологий, Московский технологический университет, просп. Вернадского, 86, Москва, Российская Федерация, 119571
E-mail: koshelevsan4es@ya.ru

Анатолий Александрович Ищенко *

Кафедра аналитической химии, Институт тонких химических технологий, Московский технологический университет, просп. Вернадского, 86, Москва, Российская Федерация, 119571
E-mail: aischenko@yasenevo.ru *

Прямое исследование и понимание динамики химических и биологических процессов, происходящих в конденсированных средах, в настоящее время находится на ранней стадии. Прогресс в этой области был вызван разработкой методов исследования структурной динамики материи в состоянии, далеком от равновесия, включая экстремальные состояния. Представленная информация служит основой для тестирования новых теоретических подходов к описанию вещества в причинно-связанной триаде «структура-динамика-свойство». Наблюдение динамического поведения материи в пространственно-временном континууме на сверхкоротких временных масштабах является необходимым первым шагом в объяснении и, в конечном счете, контроле неравновесных процессов и функциональности исследуемых систем. Метод сверхбыстрой электронной кристаллографии позволяет исследовать переходные неравновесные структуры, которые дают решающую информацию о структурной динамике фазовых переходов и когерентной динамики ядер в твердом состоянии, на поверхности и в макромолекулярных системах. В последние годы длительность электронного импульса в аппаратуре сверхбыстрой электронной дифракции значительно уменьшилась, а ускоряющее напряжение значительно увеличилось. В результате, были получены фемтосекундные импульсы электронов. Предложен метод радиочастотной группировки электронов для увеличения яркости электронного импульса. Для увеличения пространственной когерентности использовался метод электронной полевой эмиссии, а для уменьшения рассогласования скоростей светового и электронного импульсов и сжатия электронных сгустков применялось пондеромоторное волновое фронтальное ускоре-

ние. Эти достижения открыли новые возможности для изучения когерентной структурной динамики - атомно-молекулярного кино с фемтосекундным временным разрешением. В обзоре цитируются результаты нескольких всемирно известных исследовательских групп.

Ключевые слова: сверхбыстрая электронная кристаллография, промежуточные неравновесные структуры, поверхности и кристаллы, когерентная структурная динамика, динамика реакции с атомным разрешением, фемтосекундная спектроскопия

ULTRAFAST ELECTRON CRYSTALLOGRAPHY AND NANOCRYSTALLOGRAPHY: FOR CHEMISTRY, BIOLOGY AND MATERIALS SCIENCE. PART I. ULTRAFAST ELECTRON CRYSTALLOGRAPHY

L. Schafer, Y.I. Tarasov, A.V. Koshelev, A.A. Ischenko

Lothar Schafer

Department of Chemistry and Biochemistry, University of Arkansas, Fayetteville, AR 72701, USA
E-mail: schafer@uark.edu

Yury I. Tarasov

Department of Physics and Technical Mechanics, Moscow University of Technology, Institute of Fine Chemical Technologies, Vernadskogo ave., 86, Moscow, 119571, Russia
Joint Institute for High Temperatures of the RAS, Izhorskaya st., 13, bldg. 2, Moscow, 125412, Russia
E-mail: y.i.tarasov@mitht.org

Aleksandr V. Koshelev

Department of Analytical Chemistry, Moscow University of Technology, Institute of Fine Chemical Technologies, Vernadskogo ave., 86, Moscow, 119571, Russia
E-mail: koshelevsan4es@ya.ru

Anatoly A. Ischenko *

Department of Analytical Chemistry, Moscow University of Technology, Institute of Fine Chemical Technologies, Vernadskogo ave., 86, Moscow, 119571, Russia
E-mail: aischenko@yasenevo.ru *

The direct probing and understanding of the dynamics of chemical and biological processes occurring in condensed matter, is currently in its early stages. Progress in this field has been pushed by the development of methods for the study of the structural dynamics of matter in a state far from equilibrium, including extreme states. The forthcoming information serves as the basis for testing new theoretical approaches to the description of the substance in casually connected triad "structure-dynamics-function". Observation of the dynamic behavior of matter in the space-time continuum on ultrashort time scales is a necessary first step in the explanation and, ultimately, control of far from equilibrium processes, and functionality of the systems studied. The method of ultrafast electron crystallography (UEC) makes it possible to investigate transient nonequilibrium structures, which yield decisive information about the structural dynamics of the phase transitions and coherent dynamics of the nuclei in the solid state, on the surface, and in macromolecular systems. In recent years, the electron bunch path length in the UEC apparatus diminished significantly, while the accelerating voltage increased considerably. Therefore, femtosecond electron pulses were obtained. A technique of radio frequency grouping of electrons was proposed to increase the electron pulse brightness. The method of electron field emission was used to increase the spatial coherence, and ponderomotive wave front acceleration was applied to reduce the mismatch between the velocities of the light and electron pulses and to contract the electron bunches. These achievements have opened up new possibilities for studying the coherent structural dynamics – atomic and molecular movie with femtosecond temporal resolution. The results of several internationally renowned research groups are included and cited.

Key words: ultrafast electron crystallography, transient nonequilibrium structures, surfaces and crystals, coherent structural dynamics, atomically resolved reaction dynamics, femtosecond spectroscopy

Izv. Vyssh. Uchebn. Zaved. Khim. Khim. Tekhnol. 2017. V. 60. N 5

5

INTRODUCTION

The direct probing and understanding of the dynamics of biological, chemical processes, and processes occurring in solids (e.g., transport in metals, their alloys, rectification effects in semiconductors, magnetoresistance etc), which are amenable to study in real time, is currently in its early stages. Progress in this field has been pushed by the development of methods for the study of the structural dynamics of matter in a state far from equilibrium, including extreme states. The forthcoming information serves as the basis for testing new theoretical approaches to the description of the substance in casually connected triad "structure-dynamics-function". Observation of the dynamic behavior of matter in the space-time continuum on ultrashort time scales is a necessary first step in the explanation and, ultimately, control of far from equilibrium processes, and functionality of the systems studied.

The natural time scale of dynamic processes depends on the energy and length scales of the phenomenon of interest. For example, from attosecond to femtoseconds advancing time-resolved and control techniques from the molecular to the electronic time-scale; from femtoseconds to picoseconds for atomic, molecular dynamics relevant to chemistry; from picoseconds to nanoseconds for ferroelectric, magnetic diffusion, and polarization processes; from nanosecond and longer for nucleation, cellular functions, and growth of crystals. The corresponding natural length scale for these dynamic processes are in the range of atomic and molecular scale 0.1-10 nm for chemistry and biology, up to the micron scale of interactions between biological cells in grains and metal alloys.

A full description of the temporal sequence and interaction of dynamic characteristics requires the integration of information from different instrumental methods based on different physical principles, first and foremost, diffraction and spectroscopic methods with a time resolution and spatial resolution allowing the study to limit of the coherent dynamics of matter.

The quest to observe transient molecular structures and the chemical dynamics of molecules during reactions is greatly aided by employing two vantage points: the traditional spectroscopic view, which relies on the observation of energy levels and their populations, and a diffraction view, which directly images molecular structure (see more detailed discussion of this issue in the works [1-9]. Already in the 1980's, the diffraction paradigm was formulated: implementing electron diffraction with time resolution adds a temporal coordinate to the determination of molecular structures [10-13]. Time-resolved electron diffraction (TRED) rested on the concept of flash photolysis originally proposed by Norrish and Porter in 1949 [14]. Very recent advances in the generation of x-ray pulses have made possible the closely related time-resolved x-ray diffraction (TRXD). In both methods, short laser pulses create the transient structures and induce chemical dynamics that are subsequently imaged by diffraction at specific "points" in time.

The use of pico- or femtosecond bunches of electrons as probes, synchronized with the pulses of the exciting ultrashort laser radiation, led to the development of ultrafast electron crystallography and nanocrystallographic techniques [15], of dynamic transmission electron microscopy [1-3, 16, 17], to femtosecond electron diffraction of structural transitions [18] and of molecular quantum state tomography [19, 20]. One of the promising applications, developed by the electron diffraction methods, is their use for the characterization and the "visualization" of processes, occurring in the photo-excitation of free molecules and biological objects for the analysis of different surfaces, thin films, and nanostructures (see the recent review articles [6, 9, 21-37]). The combination of state-of-the-art optical techniques and diffraction methods, using different physical principles but complementing each other, opens up new possibilities for structural research at ultrashort time sequences. It provides the required integration of the triad "Structure-Dynamics-Function" in chemistry, biology, and materials science [1, 2, 5, 6, 8, 9, 38-40].

Since the 1980s, scientific laboratories around the world have begun to develop a new field of the research aimed at this goal. "Atom-resolved-molecular movies" will allow visualization of coherent dynamics of the nuclei in the molecules and fast processes in

chemical reactions in real time. Modern femtosecond laser sources have made it possible to significantly change the traditional approaches using continuous electron beams, to create ultrabright pulsed photoelectron sources, to catch ultrafast processes in the matter initiated by ultrashort laser pulses and to achieve high spatio-temporal resolution to imaging molecular processes. Ultrafast laser spectral and electron diffraction methods complement each other and open up new possibilities in chemistry and physics to light up atomic and molecular motions involved in the primary processes governing structural transitions.

Ultrafast Electron Crystallography (UEC) is an extremely powerful tool for the investigation of the transient non-equilibrium structures. These studies provide rather important information on the phase transitions and coherent dynamics of the nuclei in the solid state. In the past few years UEC was widely used also for study of structural dynamics in different nanostructures. This variation of the technique is usually referred to as UEnC (Ultrafast Electron nano-Crystallography [5, 6, 15, 21, 22, 27].

The article discusses the application of time-resolved electron diffraction to investigate condensed matter and includes the discussion of the experimental techniques, the theory of both UEC (Part I) and UenC Part II), and some of the prominent results on the study of the structural dynamics of the surface, different phase transitions in the nanoparticles, and the dynamics of the molecular assemblies. By providing high spatial resolution (down to a few hundredths or thousandths of angstrom) and high temporal resolution (in pico-femtosecond range) it is possible to observe the structural dynamics and the energy flow in condensed matter in real time.

1. EXPERIMENTAL SETUPS

Schematic diagram of UEC experimental setup is shown in Fig. 1 [1, 41].

The experimental setup consists of three ultrahigh vacuum chambers with an electron source, LEED (Low-Energy Electron Diffraction) and Auger spectrometers and a batch box of gas that allows to controls the preparation of a clean surface (see, e.g., [42]), its state during the adsorption of the atoms and the molecules and to determine the nature of its binding to the
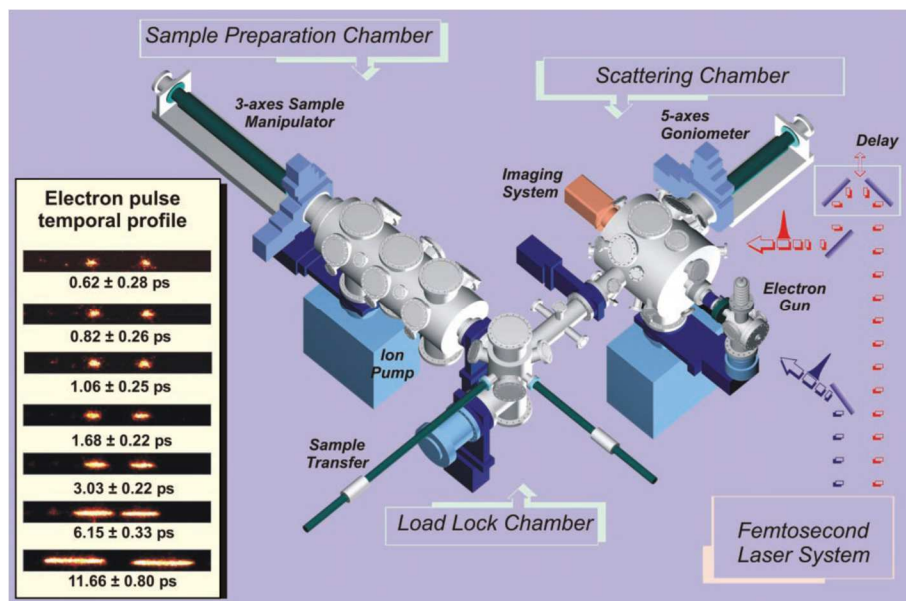

Fig. 1. Schematic diagram of the ultrafast electron crystallography experimental setup. The insert on the left shows the images of the electron beam obtained by the camera with the linear sweep [1,41]
Рис. 1. Схема экспериментальной установки для сверх-быстрой электронной кристаллографии. На вставке слева изображены электронные сгустки, полученные при работе установки в режиме камеры с линейной разверткой [1,41]

surface (chemisorption or adsorption). The device is equipped with a goniometer with an angular resolution of 0.005° and a cooling system capable of reaching temperatures of down to ~110 K. The accuracy of the internuclear distances is ~ 0.01 Å, while the maximal resolved distance is about 50 Å. Here the laser pulse duration is ~120 fs with the penetration depth of the laser radiation being of 4 nm at 266 nm and 7 µm at 800 nm.

In the laboratory of prof. Ruan at the Michigan State University (USA) it has been used the latest achievements in the field of the generation, the control and the detection of ultrashort electron pulses for UEC-researches with sub-picosecond time resolution [15]. The apparatus is shown in Fig. 2. It consists of a femtosecond laser and electron gun with silver photocathode (thickness of silver layer is 40 nm). Here 800-nm laser radiation is utilized for the photo-excitation of the sample, while 266-nm-pulses are used to generate electron bunches from the cathode. Since the laser pulse (266 nm) that initiates the photoemission of the electrons is obtained by splitting of the radiation from the same laser setup, the temporal jitter between the exciting and the probe pulses is determined by the temporal interval of the photoemission process and, in principle, has a femtosecond level or below [43]. The arrival of the probing electron bunch with respect to the pump pulse is controlled by the optical delay line that allows observe the dynamics of the photo-induced reaction. The

laser system (Ti: Sapphire laser with regenerative amplification from Spectra Physics) produced 45 fs laser pulses at 800 nm with an energies of up to 2.5 mJ and a repetition rate of 1 kHz. Using the frequency doubling or tripling, it is possible to get the 400-nm, or 266-nm pulses with the energies of up to 250 mJ and 40 mJ, respectively, which can also be utilized as a pump pulse.

electrons in the bunch) and to observe, in principle, the diffraction pattern in UEC using a single electron pulse. Note, that in UEC it is sufficient to have about 10^3 e$^-$/pulse at the pulse repetition rate of 1 kHz.

Fig. 3. Measurement of the size of the electron beam near the sample: the method of "knife edge" is shown in the insert [15]
Рис. 3. Измерение размера электронного пучка вблизи образца: метод «острия ножа» изображен на вставке [15]
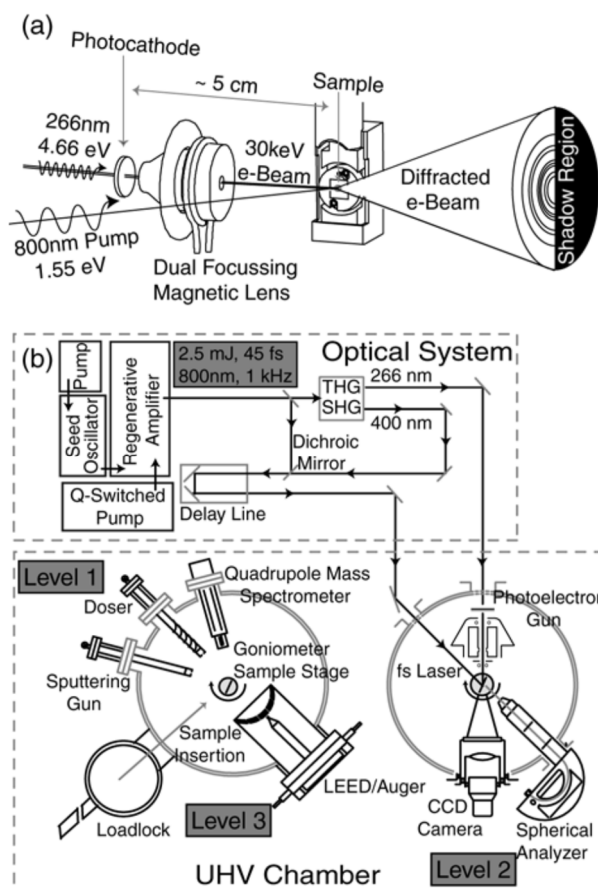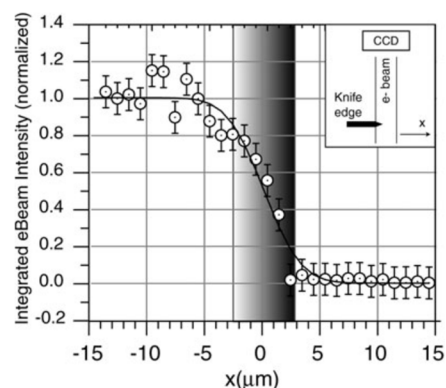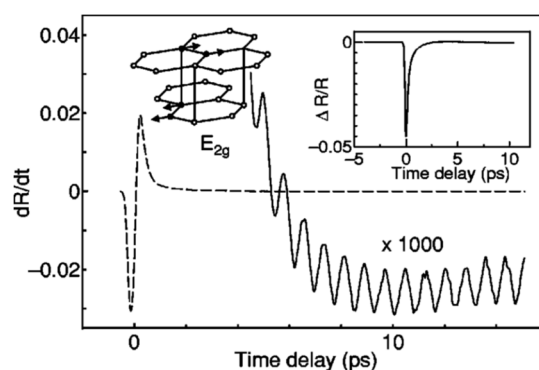

Fig. 2. UEC experimental setup. (a) The experimental arrangement of the type of "laser pump - electron probe". (b) The main parts of the high-vacuum chamber with the optical paths of femtosecond laser radiation (see text) [15]
Рис. 2. Экспериментальная установка для сверхбыстрой электронной кристаллографии. (a) расположение частей для эксперимента «лазерная накачка – электронная диагностика». (b) Компоновка основных частей в высоковакуумной камере с оптической частью для ввода излучения фемтосекундного лазера (см. текст) [15]

Fig. 4. Coherent oscillations of the intensity of reflection (dR/dt) which corresponds to inter-planar vibrations of pyrographite layers (E_{2g}). The dashed line shows the full pump and probe signal measured using the modulation technique with temporal delay. The solid line corresponds to a magnification of 1,000 times. The inset shows the profile of the main (non-modulated) pump and probe signals; here $\Delta R/R$ is the relative change in the reflection [45]
Рис. 4. Когерентные осцилляции интенсивности отражения (dR/dt), соответствующие межплоскостным колебаниям сдвига слоев (E_{2g}) пиролитического графита. Пунктирной линией показан полный сигнал «накачка-диагностика», измеренный с помощью техники модуляции с задержкой по времени. Сплошная линия соответствует тысячекратному увеличению. На вставке показан профиль основных (немодулированных) сигналов «накачка-диагностика»; здесь $\Delta R/R$ – относительное изменение интенсивности отражения [45]

The photocathode generates the electron pulses with kinetic energy of 30 keV (anode extraction field is about 6.5 kV/mm), which pass through the apertures and magnetic lenses and focused to the diameter of 5 microns (Fig. 3) on the sample located at a distance of 5 cm from the photoelectron source.

The first short-focused femtosecond photoelectron gun was designed in Miller's group [18]. It allowed to achieve high electron density (of up to 10^4

The efforts of Ruan's group [15] were trained on the focusing of the electron pulsed beam to a diameter of about 1 μm while maintaining femtosecond temporal resolution in order to reduce the mismatch of the velocities of the light and the electrons [44]. Such way ultimately allowed study individual (isolated) nanoparticles with high spatio-temporal resolution.

To demonstrate the possibilities of the existing apparatus, the photo-excitation of highly-ordered pyrolytic graphite (HOPG) has been studied. In HOPG, the phonon mode E_{2g} corresponds to the inter-planar oscillations of the shear of graphite layers (Fig. 4). It is known that these oscillations interact strongly with the femtosecond laser field [45, 46].

After the photo-excitation, it is possible to observe the generation of surface charges a subpicosecond time scale (Fig. 5). The oscillations are associated with the charge accumulation on the outside surface of pyrographite and are caused by photo-induced electron tunneling through a potential barrier from the substrate surface which is followed by the formation of two-dimensional (2D) electron gas. In this case, the positively-charged ions remain behind the photo-excitation area. The dynamics of the surface charges is closely linked to the characteristics of the charge transfer in the direction perpendicular to the basal plane of graphite and is modulated by the surface phonons. This optically-induced charge redistribution and the corresponding atomic rearrangements are discussed in Sect. 3.
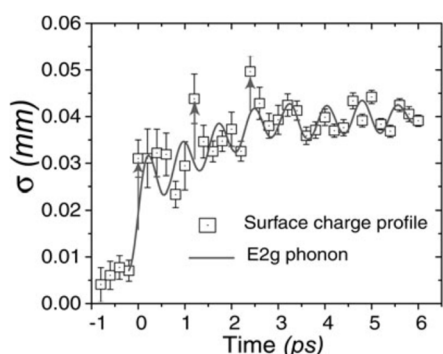

Fig. 5. Discovery of femtosecond jumps of the surface charges of Highly-Ordered Pyrolytic Graphite (HOPG) after the photo-excitation. Solid line is the result of a sinusoidal approximation of E_{2g} phonon mode oscillation with a period of 0.78 ps, which demonstrates sub-picosecond resolution of UEC experimental setup [15]

Рис. 5. Обнаружение фемтосекундных скачков поверхностных зарядов в высокоупорядоченном пиролитическом графите (HOPG) после фотовозбуждения и их последующие осцилляции. Сплошная линия представляет собой результат синусоидальной аппроксимации фононной моды E_{2g}) с периодом 0.78 пс, что является демонстрацией суб-пикосекундного разрешения, обеспечиваемого экспериментальной установкой [15]

The high-vacuum chamber is equipped with a device for sample transfer, installation, and the special devices for its characterization and purification, as shown in Fig. 2b. To maintain a high vacuum, the special additional chamber has been built in the setup which made it possible to transfer the sample into high vacuum directly from the storage area.

The acquisition of the diffraction patterns was performed using a highly sensitive CCD – camera ca-

pable of detection of single electrons. For precise control of the sample temperature and its position, five-axle goniometer has been utilized. Here the temperature was changed in the range from 20 K to 300 K. The substrate of HOPG was located directly above the calibration sample for the adjustments of the pump-probe pulses *in situ*, both in space and in time. For the cleaning and the preparation of the surface a spray gun, telephocal IR lamp and the batch gas box has been utilized. For the characterization of the sample a quadrupole mass spectrometer and LEED / Auger – system have been employed. Some of the experimental results are presented in Sect. 2 and 3.
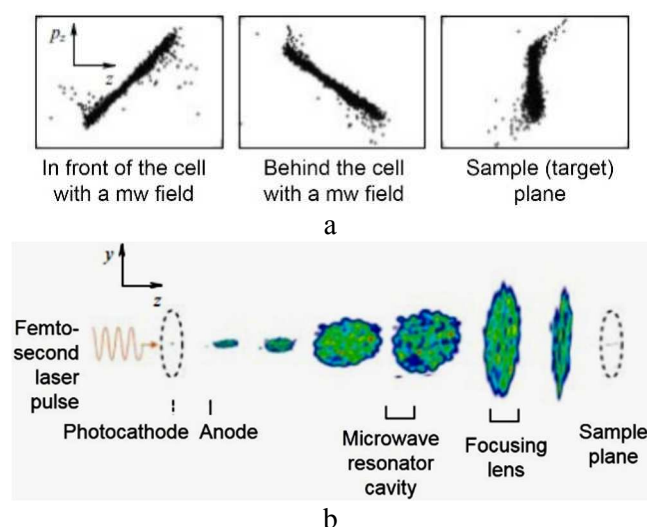

Fig. 6. (a) The principle of electron pulse injection and pulse compression in a microwave resonator. (b) Electron beam dynamics before and after passage through the microwave resonator cavity. Modeling for 104 electrons with an energy of 30 keV [48]

Рис. 6. (a) Принцип инжекции и сжатия электронных импульсов в микроволновом резонаторе. (b) Динамика электронного сгустка до и после прохождения через полость микроволнового резонатора. Моделирование выполнено для 104 электронов с энергией 30 кэВ [48]

A significant improvement in time resolution of UEC which is required for the study of ultrafast processes after the photo-excitation can be achieved by using the radio-frequency (rf) compression of the electron pulses (Fig. 6). The Institute of Nuclear Physics (Novosibirsk, Russia) together with the Max Planck Institute (Garching, Germany) has designed the ultrafast electron diffraction setup [47]. The temporal resolution of this setup can be ~10 fs. To produce electron bunches with this duration, a scheme containing a diode electron gun with a photocathode and rf resonator is proposed. Electrons, emitted from the photocathode by a laser pulse, are at first accelerated by dc voltage of 20-40 kV. The given estimates have shown that, due to the initial scatter of electron velocities on the cathode, the pulse duration at the output from the diode gun

(700-800 fs) is about of one order of the magnitude higher than that of the laser pulse (60 fs). The electron pulse formed in this way arrives into the resonator, where the electron velocities are modulated.

The amplitude of rf oscillations in the resonator was selected such that the electron pulse was grouped at the distance of 100 to 200 mm from the cavity. The working frequency of this rf cavity was selected as 6.2 GHz. In addition to the target and photocathode, a part of the laser beam is fed to the photo-detector in order to synchronize the microwave oscillations in the resonator with laser pulses. The oscillation phase stability should be about $4 \cdot 10^{-4}$ rad to achieve a 10 fs time resolution. According to the calculations, the maximal amplitude of the voltage across the resonator gap should be 3 kV. It is necessary to have a microwave signal source with a ~4W to 6W output power to obtain this voltage. The stability of amplitude oscillations in the cavity should be approximately ±0.25%.

A low-noise microwave signal source with two output frequencies (6.2 GHz and 6.1 GHz) was designed at the Research Center of the Siberian Branch of the Russian Academy of Sciences (Krasnoyarsk) to ensure the above requirements [47]. The power of the microwave signal (6.2 GHz) can be regulated in the range of 0.1-6.0 W, while the power of a 6.1 GHz frequency signal is > 5 mW. To obtain a low phase noise level and simultaneously ensure electron frequency tuning, the output signal is formed by mixing two signals, i.e., a signal of the generator across the dielectric resonator (*GDR*) and a signal of the generator controlled by voltage (*GCV*). The frequency is tuned by the *GCV*, which also has a low phase noise level at its fundamental frequency. In the scheme the power is controlled by changing a gain of the preliminary stage of the amplifier.

For the convenience of its operation, the device has an output signal power-meter and the frequency-meter, which shows the frequency detuning of the output signal from the rated value. As is known, *GDR* features a low phase noise level of about – (95-100) dB/Hz, when the offset from the carrier is 10 kHz. In the designed scheme, in order to obtain a lower phase noise-level, *GDR* is synchronized by a 100 MHz reference signal using the phase-lock (*PL*). The synchronization circuit is based on sampling of the *GDR* signal by the short pulses formed from the reference signal with a low phase noise level in the stroboscopic phase detector (*SPD*). The signal from *SPD* arrives through the low-pass filter (*LPF*) and an amplifier (PL loop filter) at the control input of the generator and finely adjusts its frequency and simultaneously compensates the phase noises of the generator. As a result, it was possible to decrease the noises

down to – (115-120) dB/Hz, when the offset from the carrier was 10 kHz. This setup for the preparation of femtosecond electron bunches was supplied to the Max Plank Institute (Garching, Germany). Using such scheme the first experiments were performed and the first results were obtained [47].

2. STRUCTURAL DYNAMICS IN CONDENSED PHASE

The method of ultrafast electron crystallography makes it possible to obtain the information about the dynamics of coherent structures in the photo-induced phase transitions in nanoparticles and macromolecules, on the solid surfaces, in thin films and the interfacial areas. It allows explore the dynamic processes at the level of the constituent elements [1, 15, 41, 49-51].

30-keV electron beam with the corresponding wavelength of ~ 0.07 Å (the wave vector is labeled as k_i) is projected at the angle of $\theta < 5°$ on the crystal surface with adsorbed atoms. The resulting diffraction pattern gives information about the structure of the surface defined by both the substrate and the adsorbed particles. Here Ruan with the co-workers [50] changed temperature of the substrate using 800-nm 120-fs laser pulses. The reference point when the pump and the probe pulses hit the surface of the crystal simultaneously was defined as time-zero $t_{z0} = 0$ (see the inset in the upper left of Fig. 3.7). Note, that the apparatus (Fig. 3.1) was pumped down to about 10^{-10} Torr. The recorded diffraction patterns, $\Delta I(\theta_i, s; t_{ref}, t)$, are the difference curves related to the underlying structure of the transient state:

$$\Delta I(\theta_i, s; t_{ref}, t) = I(\theta_i, s; t_{ref}) - I(\theta_i, s; t), \quad (1)$$

since the reference time t_{ref} can be selected either before or after the arrival of the exciting pulse. It is clear, that the diffraction pattern reveals the structure in the reciprocal space, after Fourier transformation.

The scattering intensity $I(\theta_i, s; t)$ in Eq. 1 in the kinematic approximation can be represented as follows [51]:

$$I(\theta_i, s; t) = |\Phi_H \Phi_V F_B|^2 + |\Phi_H F_S|^2 + \Phi_H \Phi_V \Phi_H (F_S F^*_B + F_B F^*_S), \quad (2)$$

where there is an explicit dependence on the scattering angle and the spatio-temporal changes. The phase coherence is also evident. For example,

$$\Phi = \sum \exp(-i \, s \, r), \quad (3)$$

where, for Φ_H $r = na + mb$, but for Φ_V $r = lc$.

The structural factors of the unit cell F are defined as follows:

$$F = \sum_i f_i(s) \exp(-B_i s^2) \exp(-i \, s \, r), \quad (4)$$

where B_i – Debye-Waller factors and $f_i(s)$ – atomic scattering factors.

Eq. 4 has been utilized for different values of θ_i and t in order to reproduce correctly the diffraction data and the rocking curves. Here it was taken into account the surface potential and the finite length of the coherent scattering of the electrons (see Sect. 3). In the structural analysis, the difference method is utilized which eliminates the influence of the scattering intensity from the ground state as well as the incoherent nuclear scattering, the inelastic scattering and the volume resonance [52].

In the reciprocal space for 2D monolayer of atoms the diffraction "rods", separated by a distances of a and b (Fig. 7), are observed. These rods correspond to the constructive interference of coherent waves. As the monolayer is embedded in a crystalline substrate, the rods in the diffraction pattern are changing due to the modulation of the distance between the planes (Fig. 7). For the electrons, the Ewald spheres defined by the vector $\boldsymbol{k}_i$, have rather large sizes, and the diffraction pattern, which is dependent on θ_i, has the bands at small scattering angles and correspondingly the Bragg spots at large scattering angles in the Laue zones.

The reflections reveal the static structure of both the surface and the lattice. But with high temporal resolution it becomes possible to carry out the additional impressive measurement. First, one can diagnose the structural changes of the surface layer and its re-structuring in real time. Secondly, there is a significant difference of the characteristic temporal scales for the processes occurring in the surface layer and in the orthogonal direction. Thus, it is possible to isolate and diagnose the initial non-equilibrium structures (but not the structures that arise during the propagation of the exciting pulse). Third, if the surface is used as the matrix, one can investigate the strengthening of the mutual influence of the substrate and the lattice and represent the structural dynamics of the process. The detailed theory of UEC is presented in the papers [53-55].
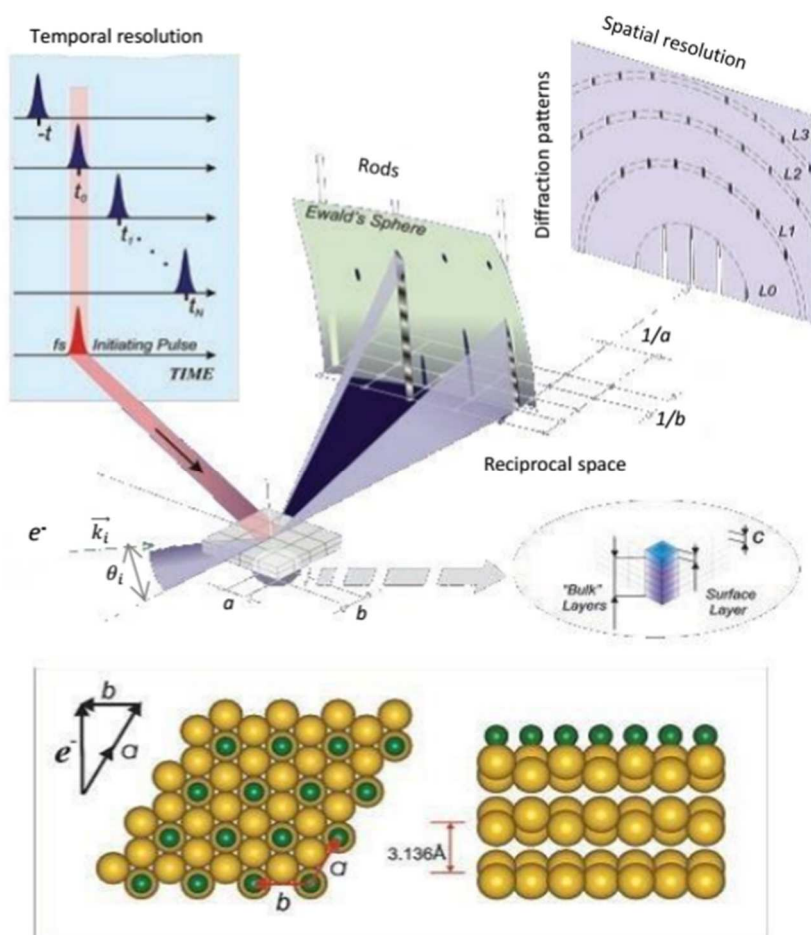

Fig. 7. Schematic diagram of ultrafast electron crystallography. Electron beam is directed to the surface of a crystal Si (111) at an angle of θ <5 °. The Ewald spheres and Laue zones (L0, L1, ...) are depicted (see text). The lower part of the figure shows the structure and the distance between the bilayers (3.136 Å). On the surface layer, the adsorbed atoms or molecules are presented [1,41,50]

Рис. 7. Схема метода сверхбыстрой электронной кристаллографии. Электронный сгусток направлен на поверхность кристалла Si (111) под углом θ<5°. На рисунке показаны сферы Эвальда и зоны Лауэ (L0, L1, …) (см. текст). На нижнем фрагменте рисунка изображена структура и расстояние между бислоями (3.136 Å), а также представлены атомы или молекулы, адсорбированные поверхностным слоем. [1,41,50]

2.1. SURFACES AND CRYSTALS

Vigliotti with the colleagues have performed an investigation of the structural dynamics of crystalline GaAs surface after the rapid increase of its temperature [56]. Using the changes in Bragg diffraction (a shift, a line width and an intensity) it has been shown, that "contraction" and "expansion" occur from -0.01 Å to +0.02 Å and that "transient temperature" (its precise definition is not given in the above-mentioned paper) reaches its maximal value of 1565 K after 7 ps (Fig. 8). The structural changes are delayed from the increase in temperature, which is demonstrated by the evolution of non-equilibrium structures.
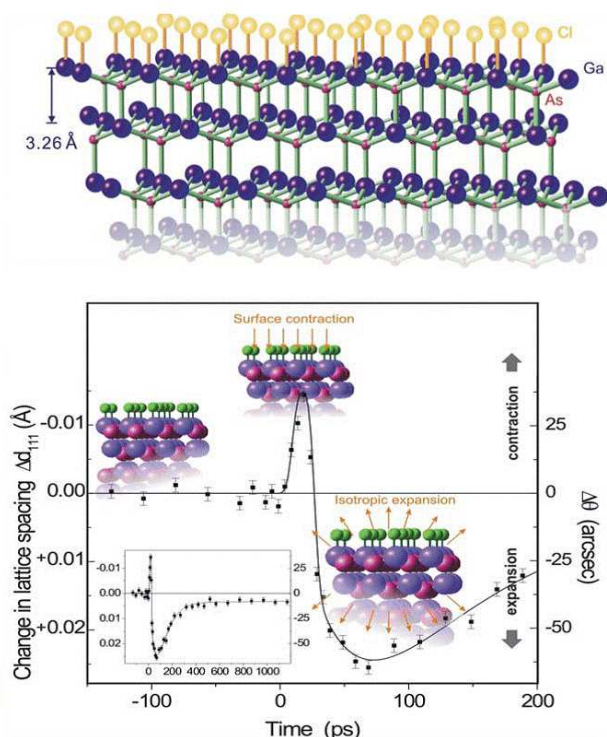

Fig. 8. Study of the surface of the crystal GaAs, covered with chlorine atoms. Only the changes in the equilibrium position of the lattice parameters are shown (see text). From the paper [1]
Рис. 8. Исследование поверхности кристалла GaAs, покрытой атомами хлора. На рисунке изображены только изменения параметров решетки относительно равновесных (см. текст). Из статьи [1]

These results [1] were compared with non-thermal femtosecond optical sensing [57]. Here GaAs surface was covered with a monolayer of chemically bound chlorine atoms. On ultra-short time scales, the contraction followed by the expansion was observed, which was caused by the increase in temperature of the phonons. On larger time scales there was observed the restructuring and the corresponding evolution towards the equilibrium structure. The registered structural dynamics can be divided into three modes: the changes, which include electron redistribution without the motion of the nuclei (from femtoseconds to a few picoseconds), coherent non-equilibrium lattice expansion (starting from 7 ps), the restructuring and the diffusion of heat (from 50 ps to several nanoseconds).

Similar studies were performed for silicon crystals in the presence and in the absence of adsorbates. The selection of the ground state as the reference point showed the changes in the structure caused by the initial femtosecond pulse, compared with the sample in the ground state at "negative" temporal delay (Fig. 8). The structural dynamics was manifested by the temporal shift on the rocking curve of the Bragg in-phase peak, while the increase in the amplitude of the corresponding oscillations was displayed in the broadening of the peaks.

Just as in the case of GaAs there was observed the motion of whole surface and bulk atoms [50]. Following the increase of the electron temperature which occurs on a femtosecond time scale, the population of optical phonons is rising, which, after a picosecond temporal delay causes acoustic waves (expansion and contraction of the lattice), and, finally, the heating of the lattice. Thus, UEC makes it possible to investigate the ultrafast dynamics of the surfaces and bulk atoms and to observe the structural changes and heat diffusion over longer temporal intervals.

2.2. CONVERSION OF GRAPHITE INTO DIAMOND

The conversion of graphite into diamond using different nano-carbon materials is of great particular interest. Such process is believed to be associated with an intermediate state of the rhombohedral phase of graphite [58, 59]. While these two forms of graphite are energetically almost degenerate, they are separated by a large energy barrier [58, 60]. Thermodynamically, these transitions can occur only under very high temperatures and pressures. Recently performed theoretical studies have shown the possibility of reducing the energy barrier by doping of graphite with charged particles [60], or by electronic excitation [46]. This was demonstrated experimentally: the formation of nano-diamonds was observed at ambient temperatures by projecting a beam of argon ions with high charge (Ar^{8+}) on graphite following the charge injection from the tip of a scanning tunneling microscope [61].

Raman et al. investigated the possible paths of photo-induced lattice motion in pyrographite using UEC [62]. Remember, that highly-oriented pyrographite consists of 2D graphite micro-domains with randomly-oriented basal planes. The excitation laser pulse had its maximum at 800 nm.

This excitation is associated with shear oscillation of the E_{2g} phonon mode [45] and can cause a change in the symmetry of the hexagonal graphite layers (ABAB) into the rhombohedral layers (ABCABC), which is required for the formation of sp^3 bonds between the layers [63]. The diffraction pattern of the pyrographite ground state consists of (006), (008), (0010) and (0012) Bragg peaks. The analysis of time-dependent scattering intensities showed that the thermalization time is ~ 8 ps which corresponds to the relaxation of the excess energy from the originally-populated mode E_{2g} into the thermal reservoir of the phonon vibrations [64]. The reduction of the intensities of Bragg peaks (006) and (0010) with respect to (008) and (0012) was also observed (Fig. 9), which corresponded to the decrease of the lattice constant by a factor of two. This was accompanied by the formation of the peak at $r = 1.9$ Å on LDF (the Layer Density Function) of graphite which was due to the new distance between the layers.
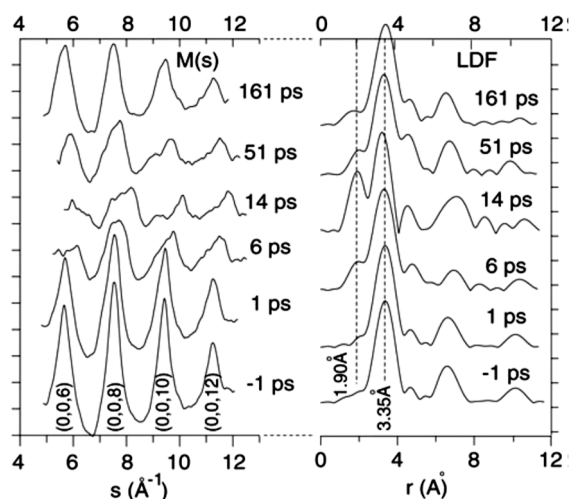

Fig. 9. The intensity of the electron scattering M(s,t) and the corresponding layer density functions (LDF) for the selected times after the rapid photo-excitation of pyrolytic graphite. The appearance of the peak at 1.90 Å indicates to the bond formation between the planes [15]
Рис. 9. Интенсивность рассеяния электронов M(s,t) и соответствующие функции плотности слоев (LDF) для некоторых моментов времени, следующих за быстрым фотовозбуждением пиролитического графита. Возникновение пика при r = 1.90 Å указывает на образование связи между плоскостями. [15]

The disappearance of the peak at long temporal delays indicates to the formation of a reversible sp^2 – sp^3 hybrid structure similar to that found in the work [65], where the graphite-diamond transformations were studied at high pressures. The process of diamond formation is likely caused by Coulomb attraction generated by photo-induced charge separation at the surface via injection of hot electrons into the surface of the substrate.

2.3. FATTY ACID CRYSTAL BILAYERS: MOLECULAR ENSEMBLES

Studies of the bilayer of fatty acids deposited onto a hydrophobic surface using Langmuir-Blodgett technique were performed using UEC. Langmuir-Blodgett technique makes it possible to control the molecular deposition of ordered molecular film layer by layer, and is rather often used for different membranes building.

Arachidic acid was used as an example. The unit cell for arachidic acid is characterized by the following set $a_0 = 4.7$-4.9 Å, $b_0 = 8.0$-8.9 Å, $c_0 = 2.54$-2.59 Å, which depends on the pH and the deposition procedure. The increase in the length of -CH_2-CH_2-CH_2- fragment by ~ 0.01 Å was experimentally observed. Fig. 10 shows the time-dependent intensity of diffraction signal.
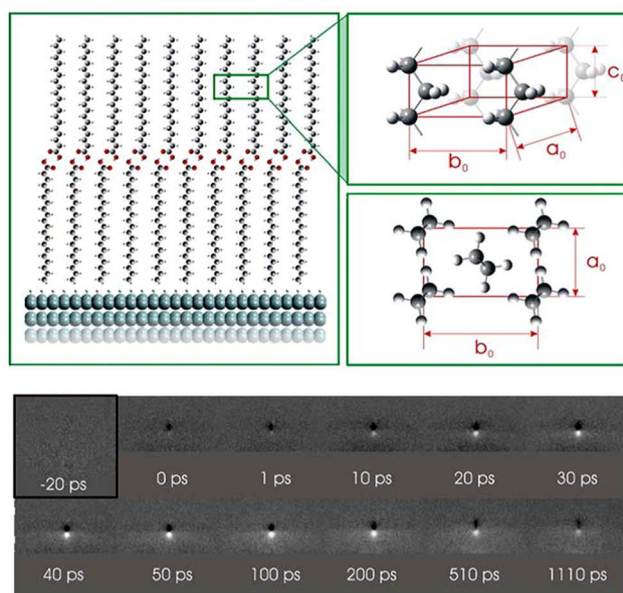

Fig. 10. Ultrafast electron crystallography of 2D bilayers of fatty acids. The structure and dynamics of the sub-cell in the temporal interval from -20 ps to 1110 ps after the laser pulse, causing heating of Si (111) substrate, is shown. UEC data represent the structural changes after 1 ps with the subsequent evolution to the equilibrium conditions [1,67]
Рис. 10. Сверхбыстрая электронная кристаллография 2D бислоев жирных кислот. На рисунке изображена структура и динамика субъячейки во временном интервале от -20 пс до 1110 пс после лазерного импульса, вызывающего нагревание подложки Si(111). Данные UEC отображают структурные изменения после 1 пс с последующей эволюцией до равновесных условий. [1,67]

Chen with the co-workers [66] investigated by UEC a single bilayer (two chains $C_{19}H_{39}COOH$) of arachidonic (eicosanoic) acid. They determined the structure and the orientation of aliphatic chains as well as the size of the molecular sub-cell (–CH_2–CH_2–). The

studies made it possible to observe the structural dynamics in the bilayer placed on the substrate, the motion of atoms and self-organization of layers [67]. Fig. 10 shows the structure of the investigated bilayer and the corresponding sub-cell in two directions.

All diffraction patterns consist of spots (and/or bands), that demonstrates a high quality of two-dimensional crystal structure of the arachidonic acid bilayer and surface of Si (111) substrate functionalized with hydrogen. The diffraction patterns at "negative time delays" and a small electron incidence angle *(at parallel and perpendicular incidence directions)* suggest that the tilting angle of chains is close to zero and the parameters of the bilayer sub-cell should be given by the set of $a_0 = 4.7$ Å, $b_0 = 8.0$ Å, $c_0 = 2.54$ Å.

The symmetry of the bilayer corresponds to rhombohedral packing R (001) with (001)-plane being parallel to the Si(111)-surface. These experimental values of the lattice parameters differ from theoretical values of $a_0 = 4.96$ Å, $b_0 = 7.4$ Å [68]. Such discrepancy can be explained by the fact that the theoretical values were calculated for infinitely-long aliphatic chains and the calculations did not take into account the terminal carboxyl group of fatty acids. Furthermore, the bilayer is consists of two monolayers, so that the substrate and the conditions of its deposition (e.g. its pressure and pH) definitely play an important role. Note, that the distance c_0 between (CH_2)-planes is in agreement with the theoretical value of 2.54 Å. In the experiment the selective structural dynamics of the bilayer was investigated. As shown in Fig. 3.10, already at the delay of about 1 ps, after the heating pulse, the weakening of the Bragg diffraction peaks was observed. The changes in the Bragg diffraction peaks become more prominent for larger temporal delays (10-100 ps). Intriguingly, both electronic and thermal pulses did not destroy the bilayer, that has been demonstrated in multiple experiments.

The observed behavior of the diffraction pattern reflects the initial stretching ($\Delta c_0 = 0.1$ Å) of the sub-cell in the bilayer induced by the heating pulse, followed by the restriction caused by heat dissipation. The stretching is taking place with the time constant of ~ 25 ps, while the subsequent contraction occurs with the time constant of ~ 55 ps. Note, that the possible compression on nanosecond temporal intervals is restructure. With 150-fs temporal resolution in the plane, perpendicular to the molecular chains, no significant changes were observed [67]. Here it should be noted that the morphology and the lattice parameters of the surface layer depend on of the matrix and the modification of the surface [69].

3. PHOTO-SWITCHED SYSTEM FROM INSULATING TO METALLIC PROPERTIES

The development of high-brightness electron sources was key to opening up this class of study. To gain some appreciation of the quality of the diffraction data that made this possible to see the dramatic improvement with source brightness [27].

Improvement in source brightness enabled a dynamic observation of the photo-induced structural changes in the interesting charge-ordered organic system comprising ethylenedioxytetrathiafulvalene (EDO-TTF) and PF_6^- counterions, $(EDO\text{-}TTF)_2PF_6$, shown in Fig. 11.

This system can be photo-switched from insulating to metallic properties [70] by means of a charge-transfer process strongly coupled to nuclear modes, stabilizing the change in charge distribution, as shown schematically in Fig. 11. Inspection of the differences between the insulating and metallic structures shows that the formation of the metallic state involves the flattening of the EDO-TTF moieties. The displacement of a bending mode toward this planar configuration would lead to an increase in the wave function overlap between molecules and increased electronic delocalization as part of the onset to metallic properties. Within a conventional transition-state picture, one would naturally expect the bending coordinate to be the dominant mode in this process. However, this simplified line of thinking only works for few atom systems. Considering just the molecules within a single-unit cell, this problem involves over 280 different degrees of freedom or dimensions. However, it was found that all of the diffraction orders could be fit by the displacement of just three reduced modes (Fig. 11C) in which the motion of the heavy PF_6^- counter-ion appears to be the key mode. In hindsight, this observation is understandable because the photo-induced change in electron distribution will lead to a change in the local field that will exert a force on the counter-ion [9, 21]. The PF_6^- ion is rather large, and its motion, through steric effects, couples the other modes. The projections along the three reaction coordinates (Fig. 11C) look like shadow projections of one another; the modes are strongly correlated.

One typically uses an approximate frozen slice of a many-body potential to discuss reaction coordinates and get a feel for the forces and types of motion involved in directing the process. However, these results show that the modes are dynamically coupled and that one cannot intuitively guess which modes are involved or the relative degree of coupling. In principle, time-dependent ab initio theory can provide the information on the relative degree of coupling between the different possible motions [9, 21]. There is a limit. Even

14

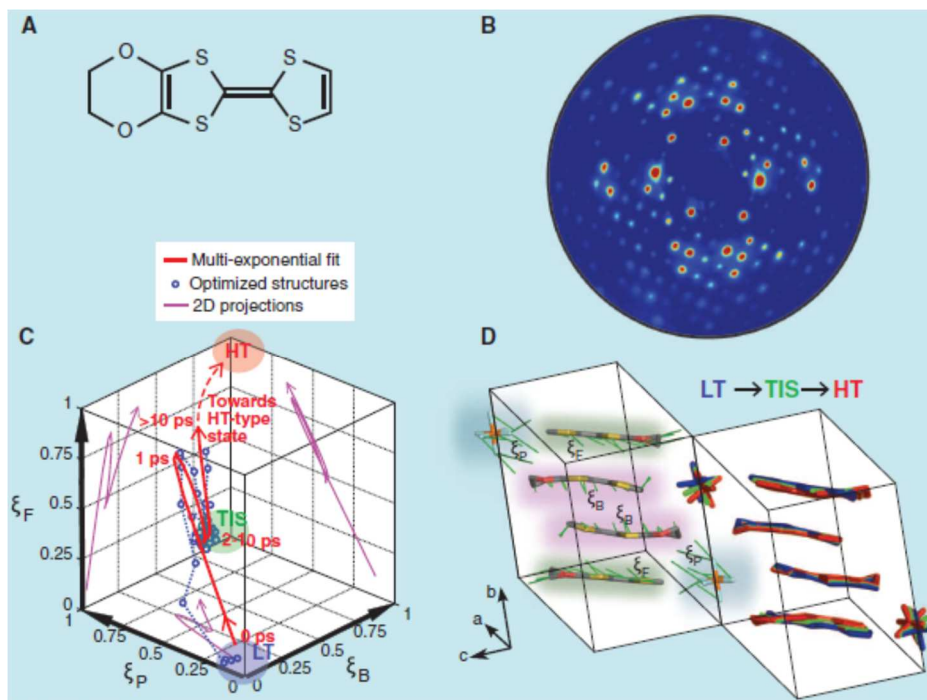Изв. вузов. Химия и хим. технология. 2017. Т. 60. Вып. 5

Fig. 11. Reduction in dimensionality. Dynamic observation of the photo-induced structural changes in the g charge-ordered organic system comprising ethylenedioxytetrathiafulvalene (EDO-TTF) and PF_6^- counter-ions, $(EDO\text{-}TTF)_2PF_6$, (A) Molecular structure of EDO-TTF. (B) Representative electron diffraction pattern to illustrate the high quality of diffraction. (C) The structural changes can be mapped onto three reduced-reaction coordinates (ξ_P, motion of the PF_6^- counter-ion; ξ_B, bending coordinate; and ξ_F, sliding motion of the rings) that stabilize the change in charge distribution, leading to electron delocalization and metallic behavior. The projections along these three normalized coordinates are highly correlated, indicating strong coupling between these nominal reaction modes. (D) Schematic depiction of the motion along these modes is given to provide a sense of the motions involved, from the insulating structure (LT), to a transient intermediate structure (TIS), to the final metallic-like structure (HT), with direction of motion indicated by the arrows and superposed structures for some sense of animation [70]

Рис. 11. Редукция размерности. Динамическое наблюдение фотоиндуцированных структурных изменений в органической системе с упорядоченным зарядом, содержащей (этилендиокси)тетратиафульвален (EDO-TTF) и противоионы PF6-, (EDO-TTF)2PF6, (A) Молекулярная структура EDO-TTF. (B) Характерная электронограмма, иллюстрирующая высокое качество разрешения. (C) Структурные изменения могут быть изображены с помощью трех координат реакции (ξ_P, движение противоиона PF_6^-; ξ_B, координата изгиба; ξ_F, скольжение колец), стабилизирующих изменение распределения заряда, приводящего к делокализации электронов и проявлению металлических свойств. Проекции вдоль этих трех нормальных координат высококоррелированы, и обнаруживают сильное взаимодействие друг с другом. (D) Схема движения вдоль трех нормальных координат приведена для изображения соответствующих типов движений, сопровождающих переход от изолированной структуры (LT) к структуре переходного состояния (TIS) и затем к финальной металлоподобной структуре (HT), причем направление движения отображено стрелками и наложенными структурами, создающими эффект анимации. [70]

the highest level of time-dependent ab initio theoretical methods have to use highly truncated model systems to approximate typical chemical reactions. In this respect, theoretical calculations of reaction coordinates are generally projected along the modes found to be most strongly coupled to the reaction coordinate. Given the level of approximations required in treating electron correlation energies and highly simplified model structures, the observed reduction in dimensionality even within full modal basis calculations might be considered to be a consequence of the truncated moiety used to model the reaction coordinate [9, 21].

We now see that this approach can be experimentally justified for even very complex systems. There is in fact an enormous reduction in dimensionality that again is the key to how chemistry reduces to transferrable concepts in the form of reaction mechanisms [27, 71].

CONCLUSION

Integration of electron optics and pulsed laser techniques into a single experimental layout provides an effective tool for research into the structural dynamics of matter with high temporal and spatial resolution. The new techniques give rise to a very promising branch of modern physics and chemistry, advancing investigations in the 4D space-time continuum for a better understanding of both the dynamic properties of molecular systems with an intricate landscape of the potential energy surface and the mechanisms holds promise to provide a common understanding of diverse phenomena from chemical/biological process to larger length scales associated with phase transitions in condensed media, including full description of nanovolumes of solid particles.

The "pump-probe" experiments using ultrashort laser pulses provide the important capabilities for the investigation of the fast processes on the surface. However, the existing experimental techniques which are based on the probe of the spectra of the adsorbed molecules provide rather limited information on the structural dynamics. Yet, the understanding of the dynamics of the surface absorbed molecules is required for a number of the applications such as heterogeneous catalysis.

The applicability of UEC and UEnC (Part II) for the study of the structural dynamics on the surfaces, the study of the influence of the adsorbed molecules, the observation of the transitions from the crystal to the liquid phases and the investigation of the surfaces with a variety of adsorbed molecules, molecular assemblies, different nanoparticles has been experimentally demonstrated. Here femtosecond laser pulses cause the coherent restructuring of the surface layers with sub-angstrom displacement of the atoms and non-equilibrium dynamics of the surface structure is determined from Bragg diffraction spots and rings.

The electron capture by the surface causes the change of the potential and subsequently affects the motion of the nuclei inside the adsorbed molecules. The adsorption of the molecules with a lower effective electronegativity leads to a decrease in the adsorption energy and reduces the characteristic time of the dynamic response of the system to the external excitation.

It was clearly demonstrated, that UEC and UEnC (Part II) can be successfully applied to study the redistribution of the charge and energy at the interfaces. For example, UEnC allows explore the samples with the surface densities as low as 6 particles per μm^2, that shows the potential possibility to observe the isolated nanoparticles. Upon reaching of the submicron transverse sizes of the probing electron bunches, it should be expected the fundamentally-new results in the field of 4D dynamics, studied with high spatio-temporal resolution.

In order to understand the underlying processes of the phase changes, it is required not only the structural imaging of the samples and their interfaces in steady conditions, but also the insight into their structural dynamics, the redistributions of their structure in real time. The development of ultrafast electron diffraction, ultrafast crystallography, ultrafast electron microscopy and the dynamic transmission electron microscopy (DTEM) allows combine atomic spatial resolution, achieved in the electron diffraction techniques, with high time resolution of the femtosecond laser experiments. In this context, the "optical pumping – electron diffraction probing" has led to an extremely powerful tool for the investigation of the structural dynamic processes in different materials.

The obtained experimental data demonstrate the capability for the direct observation of the structural dynamics of condensed phase and opens up new opportunities for the analysis of chemical substance on the surfaces in 4D space-time continuum with pico-femtosecond temporal resolution.

ЛИТЕРАТУРА

1. **Zewail A.H.** 4D ultrafast electron diffraction, crystallography, and microscopy. *Annu. Rev. Phys. Chem.* 2006. V. 57. N 1. P. 65-103.
2. **Zewail A.H.** Four-Dimensional Electron Microscopy. *Science.* 2010. V. 328. N 5975. P. 187-193.
3. **Zewail A.H., Thomas J.M.** 4D Electron Microscopy: Imaging in Space and Time. London: Imperial College Press. 2010. 360 p.
4. **Ewbank J.D., Schäfer L., Ischenko A.A.** Structural and vibrational kinetics of photoexcitation processes using time resolved electron diffraction. *J. Mol. Struct.* 2000. V. 524. N 1–3. P. 1-49.
5. **Ищенко А.А., Гиричев Г.В., Тарасов Ю.И.** Дифракция электронов: структура и динамика свободных молекул и конденсированного состояния вещества. М.: Физматлит. 2012. 616 с.
6. **Ищенко А.А., Асеев С.А., Баграташвили В.Н., Панченко В.Я., Рябов Е.А.** Сверхбыстрая электронная дифракция и электронная микроскопия: современное состояние и перспективы. *УФН.* 2014. Т. 184. Вып. 7. С. 681-722.
7. **Ischenko A.A., Aseyev S.A.** Time Resolved Electron Diffraction: for chemistry, biology and material science. San Diego: Elsevier. 2014. 310 p.
8. **Dwyer J.R., Hebeisen C.T., Ernstorfer R., Harb M., Deyirmenjian V.B., Jordan R.E., Dwayne Miller R.J.** Femtosecond electron diffraction: 'making the molecular movie'. *Phil. Trans. R. Soc. A.* 2006. V. 364. N 1840. P. 741-778.

REFERENCES

1. **Zewail A.H.** 4D ultrafast electron diffraction, crystallography, and microscopy. *Annu. Rev. Phys. Chem.* 2006. V. 57. N 1. P. 65-103. DOI: 10.1146/annurev.physchem.57.032905.104748.
2. **Zewail A.H.** Four-Dimensional Electron Microscopy. *Science.* 2010. V. 328. N 5975. P. 187-193. DOI: 10.1126/science.1166135.
3. **Zewail A.H., Thomas J.M.** 4D Electron Microscopy: Imaging in Space and Time. London: Imperial College Press. 2010. 360 p.
4. **Ewbank J.D., Schäfer L., Ischenko A.A.** Structural and vibrational kinetics of photoexcitation processes using time resolved electron diffraction. *J. Mol. Struct.* 2000. V. 524. N 1–3. P. 1-49. DOI: 10.1016/S0022-2860(99)00419-6.
5. **Ischenko A.A., Girichev G.V., Tarasov Y.I.** Electron diffraction: structure and dynamics of free molecules and condensed matter. M.: Fizmatlit. 2012. 616 p. (in Russian).
6. **Ischenko A.A., Aseev S.A., Bagratashvili V.N., Panchenko V.Y., Ryabov E.A.** Ultrafast electron diffraction and electron microscopy: present status and future prospects. *Phys. Usp.* 2014. V. 57. N 7. P. 633-669. DOI: 10.3367/UFNe.0184.201407a.0681.
7. **Ischenko A.A., Aseyev S.A.** Time Resolved Electron Diffraction: for chemistry, biology and material science. San Diego: Elsevier. 2014. 310 p.
8. **Dwyer J.R., Hebeisen C.T., Ernstorfer R., Harb M., Deyirmenjian V.B., Jordan R.E., Dwayne Miller R.J.** Femtosecond electron diffraction: 'making the molecular movie'. *Phil. Trans. R. Soc. A.* 2006. V. 364. N 1840. P. 741-778.

16

Изв. вузов. Химия и хим. технология. 2017. Т. 60. Вып. 5

9. **Dwayne Miller R.J.** Mapping Atomic Motions with Ultrabright Electrons: The Chemists' Gedanken Experiment Enters the Lab Frame. *Annu. Rev. Phys. Chem.* 2014. V. 65. N 1. P. 583-604.

10. **Ischenko A.A., Golubkov V.V., Spiridonov V.P., Zgurskii A.V., Akhmanov A.S., Vabischevich M.G., Bagratashvili V.N.** A stroboscopical gas-electron diffraction method for the investigation of short-lived molecular species. *Appl. Phys. B.* 1983. V. 32. N 3. P. 161-163.

11. **Ищенко А.А., Баграташвили В.Н., Голубков В.В., Спиридонов В.П., Згурский А.В., Ахманов А.С.** Наблюдение дифракции электронов на свободных радикалах – продуктах ИК многофотонной диссоциации молекул CF$_3$I с помощью стробоскопической газовой электронографии. *Вестн. Моск. Ун-та. Сер. 2: Химия.* 1985. Т. 26. Вып. 2. С. 140-143.

12. **Ищенко А.А., Тарасов Ю.И., Спиридонов В.П., Згурский А.В.** Исследование короткоживущих интермедиатов и структурной кинетики фотовозбужденных молекул с помощью стробоскопической электронографии. Сб. тр. конференции «Структура и свойства молекул». Иваново: ИХНР. 1988. С. 63-77.

13. **Вабишевич М.Г., Ищенко А.А.** А.С. 1679907 СССР. 1991.

14. **Norrish R.G.W., Porter G.** Chemical Reactions Produced by Very High Light Intensities. *Nature.* 1949. V. 164. P. 658.

15. **Ruan C.-Y., Murooka Y., Raman R.K., Murdick R.A., Worhatch R.J., Pell A.** The Development and Applications of Ultrafast Electron Nanocrystallography. *Microsc. Microanal.* 2009. V. 15. N 4. P. 323-337.

16. **Weber P.M., Carpenter S.D., Lucza T.** Reflectron design for femtosecond electron guns. *Proc. SPIE.* 1995. V. 2521. P. 23-30.

17. **King W.E., Campbell G.H., Frank A., Reed B., Schmerge J.F., Siwick B.J., Stuart B.C., Weber P.M.** Ultrafast electron microscopy in materials science, biology, and chemistry. *J. Appl. Phys.* 2005. V. 97. N 11. P. 111101, 1-27.

18. **Siwick B.J., Dwyer J.R., Jordan R.E., Dwayne Miller R.J.** An Atomic-Level View of Melting Using Femtosecond Electron Diffraction. *Science.* 2003. V. 302. N 5649. P. 1382-1385.

19. **Ischenko A.A., Ewbank J.D., Schafer L.** Structural and Vibrational Kinetics by Time-Resolved Gas Electron Diffraction: Stochastic Approach to Data Analysis. *J. Phys. Chem.* 1995. V. 99. N 43. P. 15790-15797.

20. **Ischenko A.A., Shafer L., Ewbank J.D.** Tomography of the Molecular Quantum State by Time-Resolved Electron Diffraction. *Proc. SPIE* 1999. V. 3516. P. 580-595.

21. **Sciaini G., Dwayne Miller R.J.** Femtosecond electron diffraction: heralding the era of atomically resolved dynamics. *Rep. Prog. Phys.* 2011. V. 74. N 9. P. 096101, 1-36.

22. **Ishchenko A.A., Bagratashvili V.N., Avilov A.S.** Methods for studying the coherent 4D structural dynamics of free molecules and condensed state of matter. *CryRp.* 2011. V. 56. N 5. P. 751-773.

23. **Flannigan D.J., Zewail A.H.** 4D Electron Microscopy: Principles and Applications. *Acc. Chem. Res.* 2012. V. 45. N 10. P. 1828-1839.

24. **Hada M., Pichugin K., Sciaini G.** Ultrafast structural dynamics with table top femtosecond hard X-ray and electron diffraction setups. *EPJ ST.* 2013. V. 222. N 5. P. 1093-1123.

9. **Dwayne Miller R.J.** Mapping Atomic Motions with Ultrabright Electrons: The Chemists' Gedanken Experiment Enters the Lab Frame. *Annu. Rev. Phys. Chem.* 2014. V. 65. N 1. P. 583-604. DOI: 10.1146/annurev-physchem-040412-110117.

10. **Ischenko A.A., Golubkov V.V., Spiridonov V.P., Zgurskii A.V., Akhmanov A.S., Vabischevich M.G., Bagratashvili V.N.** A stroboscopical gas-electron diffraction method for the investigation of short-lived molecular species. *Appl. Phys. B.* 1983. V. 32. N 3. P. 161-163. DOI: 10.1007/BF00688823.

11. **Ischenko A.A., Bagratashvili V.N., Golubkov V.V., Spiridonov V.P., Zgurskii A.V., Akhmanov A. S.** The observation of electron diffraction from free radicals - products of the IR multiphoton dissociation of CF$_3$I molecules by stroboscopic gas electron diffraction. *Vestn. MSU. Ser. 2. Khimiya.* 1985. V. 26. N 2. P. 140-143 (in Russian).

12. **Ischenko A. A., Tarasov Y. I., Spiridonov V. P., Zgurskii A. V.** The study of short-lived intermediate species and structural kinetics of photoexcited molecules by stroboscopic electron diffraction. The Structure and Properties of Molecules. Ivanovo: IICS. 1988. P. 63-77 (in Russian).

13. **Vabishchevich M.G., Ischenko A.A.** Method of studying the kinetics of fast processes. USSR Certificate number 1679907. 1991 (in Russian).

14. **Norrish R.G.W., Porter G.** Chemical Reactions Produced by Very High Light Intensities. *Nature.* 1949. V. 164. P. 658. DOI: 10.1038/164658a0.

15. **Ruan C.-Y., Murooka Y., Raman R.K., Murdick R.A., Worhatch R.J., Pell A.** The Development and Applications of Ultrafast Electron Nanocrystallography. *Microsc. Microanal.* 2009. V. 15. N 4. P. 323-337. DOI: 10.1017/S1431927609090709.

16. **Weber P.M., Carpenter S.D., Lucza T.** Reflectron design for femtosecond electron guns. *Proc. SPIE.* 1995. V. 2521. P. 23-30. DOI: 10.1117/12.218364.

17. **King W.E., Campbell G.H., Frank A., Reed B., Schmerge J.F., Siwick B.J., Stuart B.C., Weber P.M.** Ultrafast electron microscopy in materials science, biology, and chemistry. *J. Appl. Phys.* 2005. V. 97. N 11. P. 111101, 1-27.

18. **Siwick B.J., Dwyer J.R., Jordan R.E., Dwayne Miller R.J.** An Atomic-Level View of Melting Using Femtosecond Electron Diffraction. *Science.* 2003. V. 302. N 5649. P. 1382-1385. DOI: 10.1126/science.1090052.

19. **Ischenko A.A., Ewbank J.D., Schafer L.** Structural and Vibrational Kinetics by Time-Resolved Gas Electron Diffraction: Stochastic Approach to Data Analysis. *J. Phys. Chem.* 1995. V. 99. N 43. P. 15790-15797. DOI: 10.1021/j100043a017.

20. **Ischenko A.A., Shafer L., Ewbank J.D.** Tomography of the Molecular Quantum State by Time-Resolved Electron Diffraction. *Proc. SPIE* 1999. V. 3516. P. 580-595. DOI: 10.1117/12.350538.

21. **Sciaini G., Dwayne Miller R.J.** Femtosecond electron diffraction: heralding the era of atomically resolved dynamics. *Rep. Prog. Phys.* 2011. V. 74. N 9. P. 096101, 1-36.

22. **Ishchenko A.A., Bagratashvili V.N., Avilov A.S.** Methods for studying the coherent 4D structural dynamics of free molecules and condensed state of matter. *CryRp.* 2011. V. 56. N 5. P. 751-773. DOI: 10.1134/s1063774511050129.

23. **Flannigan D.J., Zewail A.H.** 4D Electron Microscopy: Principles and Applications. *Acc. Chem. Res.* 2012. V. 45. N 10. P. 1828-1839. DOI: 10.1021/ar3001684.

24. **Hada M., Pichugin K., Sciaini G.** Ultrafast structural dynamics with table top femtosecond hard X-ray and electron diffraction setups. *EPJ ST.* 2013. V. 222. N 5. P. 1093-1123. DOI: 10.1140/epjst/e2013-01909-9.

Izv. Vyssh. Uchebn. Zaved. Khim. Khim. Tekhnol. 2017. V. 60. N 5

17

25. **Aseyev S.A., Weber P.M., Ischenko A.A.** Ultrafast Electron Microscopy for Chemistry, Biology and Material Science. *JASMI*. 2013. V. 03. N 01. P. 30-53.

26. **Baum P.** Towards ultimate temporal and spatial resolutions with ultrafast single-electron diffraction. *J. Phys. B: At. Mol. Opt. Phys.* 2014. V. 47. N 12. P. 124005.

27. **Dwayne Miller R.J.** Femtosecond Crystallography with Ultrabright Electrons and X-rays: Capturing Chemistry in Action. *Science*. 2014. V. 343. N 6175. P. 1108-1116.

28. **Campbell G.H., McKeown J.T., Santala M.K.** Time resolved electron microscopy for in situ experiments. *Appl. Phys. Rev.* 2014. V. 1. N 4. P. 041101.

29. **Kim K.T., Villeneuve D.M., Corkum P.B.** Manipulating quantum paths for novel attosecond measurement methods. *Nat Photon*. 2014. V. 8. N 3. P. 187-194.

30. **Petek H.** Single-Molecule Femtochemistry: Molecular Imaging at the Space-Time Limit. *ACS Nano*. 2014. V. 8. N. 1. P. 5-13. DOI: 10.1021/nn4064538.

31. **Manz S., Casandruc A., Zhang D., Zhong Y., Loch R.A., Marx A., Hasegawa T., Liu L.C., Bayesteh S., Delsim-Hashemi H., Hoffmann M., Felber M., Hachmann M., Mayet F., Hirscht J., Keskin S., Hada M., Epp S.W., Flottmann K., Dwayne Miller R.J.** Mapping atomic motions with ultrabright electrons: towards fundamental limits in space-time resolution. *Farad. Discuss.* 2015. V. 177. P. 467-491. DOI: 10.1039/C4FD00204K.

32. **Robinson M.S., Lane P.D., Wann D.A.** A compact electron gun for time-resolved electron diffraction. *Rev. Sci. Instrum.* 2015. V. 86. N 1. P. 013109.

33. **Plemmons D.A., Suri P.K., Flannigan D.J.** Probing Structural and Electronic Dynamics with Ultrafast Electron Microscopy. *Chem. Mater.* 2015. V. 27. N 9. P. 3178-3192.

34. **Zhu P., Zhu Y., Hidaka Y., Wu L., Cao J., Berger H., Geck J., Kraus R., Pjerov S., Shen Y., Tobey R.I., Hill J.P., Wang X.J.** Femtosecond time-resolved MeV electron diffraction. *New J. Phys.* 2015. V. 17. N 6. P. 063004.

35. **Gerbig C., Senftleben A., Morgenstern S., Sarpe C., Baumert T.** Spatio-temporal resolution studies on a highly compact ultrafast electron diffractometer. *New J. Phys.* 2015. V. 17. N 4. P. 043050.

36. **Centurion M.** Ultrafast imaging of isolated molecules with electron diffraction. *J. Phys. B: At. Mol. Opt. Phys.* 2016. V. 49. N 6. P. 062002.

37. **Ischenko A.A., Schaefer L., Tarasov Y.I., Ryabov E.A., Aseyev S.A.** Ultrafast Transmission Electron Microscopy. *Fine Chemical Technologies*. 2017. V. 12. N 1. P. 5-25.

38. **Бучаченко А.Л.** Химия на рубеже веков: свершения и перспективы. *Успехи химии*. 1999. Т. 68. № 2. С. 99-118.

39. **Бучаченко А.Л., Бердинский В.Л.** Спиновой катализ – новый тип катализа в химии. *Усп. химии*. Т. 73. Вып. 17. С. 1123-1130.

40. **Надточенко В.А., Денисов Н.Н., Гак В.Ю., Гостев Ф.Е., Титов А.А., Саркисов О.М., Никандров В.В**. Фемтосекундная релаксация фотовозбужденных состояний наноразмерных полупроводниковых частиц оксидов железа. *Доклады АН*. 2002. Т. 62. Вып. 3. С. 457-461.

41. **Lobastov V.A., Srinivasan R., Vigliotti F., Ruan C.-Y., Feenstra J.S., Chen S., Park S.T., Xu S., Zewail A.H.** Ultrafast Electron Diffraction, in: Ultrafast Optics IV: Selected Contributions to the 4th International Conference on Ultrafast Optics. 2004. New York: Springer. P. 419-435.

42. **Оура К., Лифшиц В.Г., Саранин А.А., Зотов А.В., Катаяма М**. Введение в физику поверхности. М.: Наука. 2006. 494 с.

25. **Aseyev S.A., Weber P.M., Ischenko A.A.** Ultrafast Electron Microscopy for Chemistry, Biology and Material Science. *JASMI*. 2013. V. 03. N 01. P. 30-53. DOI: 10.4236/jasmi.2013.31005.

26. **Baum P.** Towards ultimate temporal and spatial resolutions with ultrafast single-electron diffraction. *J. Phys. B: At. Mol. Opt. Phys.* 2014. V. 47. N 12. P. 124005. DOI: 10.1088/0953-4075/47/12/124005.

27. **Dwayne Miller R.J.** Femtosecond Crystallography with Ultrabright Electrons and X-rays: Capturing Chemistry in Action. *Science*. 2014. V. 343. N. 6175. P. 1108-1116. DOI: 10.1126/science.1248488.

28. **Campbell G.H., McKeown J.T., Santala M.K.** Time resolved electron microscopy for in situ experiments. *Appl. Phys. Rev.* 2014. V. 1. N 4. P. 041101. DOI: 10.1063/1.4900509.

29. **Kim K.T., Villeneuve D.M., Corkum P.B.** Manipulating quantum paths for novel attosecond measurement methods. *Nat Photon*. 2014. V. 8. N 3. P. 187-194. DOI: 10.1038/nphoton.2014.26.

30. **Petek H.** Single-Molecule Femtochemistry: Molecular Imaging at the Space-Time Limit. *ACS Nano*. 2014. V. 8. N 1. P. 5-13. DOI: 10.1021/nn4064538.

31. **Manz S., Casandruc A., Zhang D., Zhong Y., Loch R.A., Marx A., Hasegawa T., Liu L.C., Bayesteh S., Delsim-Hashemi H., Hoffmann M., Felber M., Hachmann M., Mayet F., Hirscht J., Keskin S., Hada M., Epp S.W., Flottmann K., Dwayne Miller R.J.** Mapping atomic motions with ultrabright electrons: towards fundamental limits in space-time resolution. *Farad. Discuss.* 2015. V. 177. P. 467-491. DOI: 10.1039/C4FD00204K.

32. **Robinson M.S., Lane P.D., Wann D.A.** A compact electron gun for time-resolved electron diffraction. *Rev. Sci. Instrum.* 2015. V. 86. N 1. P. 013109. DOI: 10.1063/1.4905335.

33. **Plemmons D.A., Suri P.K., Flannigan D.J.** Probing Structural and Electronic Dynamics with Ultrafast Electron Microscopy. *Chem. Mater.* 2015. V. 27. N 9. P. 3178-3192. DOI: 10.1021/acs.chemmater.5b00433.

34. **Zhu P., Zhu Y., Hidaka Y., Wu L., Cao J., Berger H., Geck J., Kraus R., Pjerov S., Shen Y., Tobey R.I., Hill J.P., Wang X.J.** Femtosecond time-resolved MeV electron diffraction. *New J. Phys.* 2015. V. 17. N 6. P. 063004. DOI: 10.1088/1367-2630/17/6/063004.

35. **Gerbig C., Senftleben A., Morgenstern S., Sarpe C., Baumert T.** Spatio-temporal resolution studies on a highly compact ultrafast electron diffractometer. *New J. Phys.* 2015. V. 17. N 4. P. 043050. DOI: 10.1088/1367-2630/17/4/043050.

36. **Centurion M.** Ultrafast imaging of isolated molecules with electron diffraction. *J. Phys. B: At. Mol. Opt. Phys.* 2016. V. 49. N 6. P. 062002. DOI: 10.1088/0953-4075/49/6/062002.

37. **Ischenko A.A., Schaefer L., Tarasov Y.I., Ryabov E.A., Aseyev S.A.** Ultrafast Transmission Electron Microscopy. *Fine Chemical Technologies*. 2017. V. 12. N 1. P. 5-25.

38. **Buchachenko A.L.** Chemistry on the border of two centuries – achievements and prospects. *Russ. Chem. Rev.* 1999. V. 68. N 2. P. 85-102. DOI: 10.1070/RC1999v068n02ABEH000487.

39. **Buchachenko A.L., Berdinsky V.L.** Spin catalysis as a new type of catalysis in chemistry *Russ. Chem. Rev.* 2004. V. 73. N 11. P. 1033-1039. DOI: 10.1070/RC2004v073n11ABEH000888.

40. **Nadtochenko V.A., Denisov N.N., Gak V.Y., Gostev F.E., Titov A.A., Sarkisov O.M., Nikandrov V.V.** Femtosecond relaxation of photoexcited states in nanosized semiconductor particles of iron oxides. *DAN* 2002. V. 62. N 3. P. 457-461 (in Russian).

41. **Lobastov V.A., Srinivasan R., Vigliotti F., Ruan C.-Y., Feenstra J.S., Chen S., Park S.T., Xu S., Zewail A.H.**

18

Изв. вузов. Химия и хим. технология. 2017. Т. 60. Вып. 5

43. **Cavalieri A.L., Muller N., Uphues T., Yakovlev V.S., Baltuska A., Horvath B., Schmidt B., Blumel L., Holzwarth R., Hendel S., Drescher M., Kleineberg U., Echenique P.M., Kienberger R., Krausz F., Heinzmann U.** Attosecond spectroscopy in condensed matter. *Nature.* 2007. V. 449. N. 7165. P. 1029-1032. DOI: 10.1038/nature06229.

44. **Williamson J.C., Zewail A.H.** Ultrafast electron diffraction. Velocity mismatch and temporal resolution in crossed-beam experiments. *Chem. Phys. Lett.* 1993. V. 209. N 1. P. 10-16.

45. **Mishina T., Nitta K., Masumoto Y.** Coherent lattice vibration of interlayer shearing mode of graphite. *Phys. Rev. B.* 2000. V. 62. N 4. P. 2908-2911.

46. **Ishioka K., Hase M., Kitajima M., Ushida K.** Ultrafast carrier and phonon dynamics in ion-irradiated graphite. *Appl. Phys. Lett.* 2001. V. 78. N 25. P. 3965-3967. DOI: 10.1063/1.1379782.

47. **Vladimirov V.M., Zapryagaev I.A., Konnov V.G., Kurkin G.Y., Tarnetskii V.V., Chernov K.N.** A low-noise microwave signal source. *Instrum. Exp. Tech.* 2010. V. 53. N 5. P. 708-709. DOI: 10.1134/S0020441210050155.

48. **Tao Z., Zhang H., Duxbury P.M., Berz M., Ruan C.-Y.** Space charge effects in ultrafast electron diffraction and imaging. *J. Appl. Phys.* 2012. V. 111. N 4. P. 044316. DOI: 10.1063/1.3685747.

49. **Lobastov V.A., Srinivasan R., Zewail A.H.** Four-dimensional ultrafast electron microscopy. *PNAS.* 2005. V. 102. N 20. P. 7069-7073. DOI: 10.1073/pnas.0502607102.

50. **Ruan C.-Y., Vigliotti F., Lobastov V.A., Chen S., Zewail A.H.** Ultrafast electron crystallography: Transient structures of molecules, surfaces, and phase transitions. *PNAS.* 2004. V. 101. N 5. P. 1123-1128. DOI: 10.1073/pnas.0307302101.

51. **Ruan C.-Y., Murooka Y., Raman R.K., Murdick R.A.** Dynamics of Size-Selected Gold Nanoparticles Studied by Ultrafast Electron Nanocrystallography. *Nano Letters.* 2007. V. 7. N 5. P. 1290-1296.

52. **Ino S.** Experimental Overview of Surface Structure Determination by RHEED, in: Reflection High-Energy Electron Diffraction and Reflection Electron Imaging of Surfaces, 1988. Boston: Springer US. P. 3-28. DOI: 10.1007/978-1-4684-5580-9_1.

53. **Yang D.-S., Gedik N., Zewail A.H.** Ultrafast Electron Crystallography. 1. Nonequilibrium Dynamics of Nanometer-Scale Structures. *J. Phys. Chem. C.* 2007. V. 111. N 13. P. 4889-4919. DOI: 10.1021/jp067466.

54. **Tang J., Yang D.-S., Zewail A.H.** Ultrafast Electron Crystallography. 3. Theoretical Modeling of Structural Dynamics. *J. Phys. Chem. C.* 2007. V. 111. N 25. P. 8957-8970.

55. **Schäfer S., Liang W., Zewail A.H.** Structural dynamics of surfaces by ultrafast electron crystallography: Experimental and multiple scattering theory. *J. Chem. Phys.* 2011. V. 135. N 21. P. 214201.

56. **Vigliotti F., Chen S., Ruan C.-Y., Lobastov V.A., Zewail A.H.** Ultrafast Electron Crystallography of Surface Structural Dynamics with Atomic-Scale Resolution. *Angew. Chem. Int. Ed.* 2004. V. 43. N 20. P. 2705-2709.

57. **Sundaram S.K., Mazur E.** Inducing and probing non-thermal transitions in semiconductors using femtosecond laser pulses. *Nat Mater.* 2002. V. 1. N 4. P. 217-224.

58. **Fahy S., Louie S.G., Cohen M.L.** Pseudopotential total-energy study of the transition from rhombohedral graphite to diamond. *Phys. Rev. B.* 1986. V. 34. N 2. P. 1191-1199.

Ultrafast Electron Diffraction, in: Ultrafast Optics IV: Selected Contributions to the 4th International Conference on Ultrafast Optics. 2004. New York: Springer. P. 419-435. DOI: 10.1007/978-0-387-34756-1_54.

42. **Oura K., Lifshits V.G., Saranin A.A., Zotov A.V., Katayama M.** Introduction to the physics of the surface. M.: Nauka. 2006. 494 p. (in Russian).

43. **Cavalieri A.L., Muller N., Uphues T., Yakovlev V.S., Baltuska A., Horvath B., Schmidt B., Blumel L., Holzwarth R., Hendel S., Drescher M., Kleineberg U., Echenique P.M., Kienberger R., Krausz F., Heinzmann U.** Attosecond spectroscopy in condensed matter. *Nature.* 2007. V. 449. N 7165. P. 1029-1032. DOI: 10.1038/nature06229.

44. **Williamson J.C., Zewail A.H.** Ultrafast electron diffraction. Velocity mismatch and temporal resolution in crossed-beam experiments. *Chem. Phys. Lett.* 1993. V. 209. N 1. P. 10-16. DOI: 10.1016/0009-2614(93)87193-7.

45. **Mishina T., Nitta K., Masumoto Y.** Coherent lattice vibration of interlayer shearing mode of graphite. *Phys. Rev. B.* 2000. V. 62. N 4. P. 2908-2911. DOI: 10.1103/PhysRevB.62.2908.

46. **Ishioka K., Hase M., Kitajima M., Ushida K.** Ultrafast carrier and phonon dynamics in ion-irradiated graphite. *Appl. Phys. Lett.* 2001. V. 78. N 25. P. 3965-3967. DOI: 10.1063/1.1379782.

47. **Vladimirov V.M., Zapryagaev I.A., Konnov V.G., Kurkin G.Y., Tarnetskii V.V., Chernov K.N.** A low-noise microwave signal source. *Instrum. Exp. Tech.* 2010. V. 53. N 5. P. 708-709. DOI: 10.1134/S0020441210050155.

48. **Tao Z., Zhang H., Duxbury P.M., Berz M., Ruan C.-Y.** Space charge effects in ultrafast electron diffraction and imaging. *J. Appl. Phys.* 2012. V. 111. N 4. P. 044316. DOI: 10.1063/1.3685747.

49. **Lobastov V.A., Srinivasan R., Zewail A.H.** Four-dimensional ultrafast electron microscopy. *PNAS.* 2005. V. 102. N 20. P. 7069-7073. DOI: 10.1073/pnas.0502607102.

50. **Ruan C.-Y., Vigliotti F., Lobastov V.A., Chen S., Zewail A.H.** Ultrafast electron crystallography: Transient structures of molecules, surfaces, and phase transitions. *PNAS.* 2004. V. 101. N 5. P. 1123-1128. DOI: 10.1073/pnas.0307302101.

51. **Ruan C.-Y., Murooka Y., Raman R.K., Murdick R.A.** Dynamics of Size-Selected Gold Nanoparticles Studied by Ultrafast Electron Nanocrystallography. *Nano Letters.* 2007. V. 7. N 5. P. 1290-1296. DOI: 10.1021/nl070269h.

52. **Ino S.** Experimental Overview of Surface Structure Determination by RHEED, in: Reflection High-Energy Electron Diffraction and Reflection Electron Imaging of Surfaces, 1988. Boston: Springer US. P. 3-28. DOI: 10.1007/978-1-4684-5580-9_1.

53. **Yang D.-S., Gedik N., Zewail A.H.** Ultrafast Electron Crystallography. 1. Nonequilibrium Dynamics of Nanometer-Scale Structures. *J. Phys. Chem. C.* 2007. V. 111. N 13. P. 4889-4919. DOI: 10.1021/jp067466.

54. **Tang J., Yang D.-S., Zewail A.H.** Ultrafast Electron Crystallography. 3. Theoretical Modeling of Structural Dynamics. *J. Phys. Chem. C.* 2007. V. 111. N 25. P. 8957-8970. DOI: 10.1021/jp073015t.

55. **Schäfer S., Liang W., Zewail A.H.** Structural dynamics of surfaces by ultrafast electron crystallography: Experimental and multiple scattering theory. *J. Chem. Phys.* 2011. V. 135. N 21. P. 214201. DOI: 10.1063/1.3663963.

56. **Vigliotti F., Chen S., Ruan C.-Y., Lobastov V.A., Zewail A.H.** Ultrafast Electron Crystallography of Surface Structural Dynamics with Atomic-Scale Resolution. *Angew. Chem. Int. Ed.* 2004. V. 43. N 20. P. 2705-2709. DOI: 10.1002/anie.200453983.

59. **Yang G.W., Wang J.B.** Pulsed-laser-induced transformation path of graphite to diamond via an intermediate rhombohedral graphite. *Appl. Phys. A.* 2001. V. 72. N 4. P. 475-479. DOI: 10.1007/s003390000537.

60. **Nakayama H., Katayama-Yoshida H.** Direct conversion of graphite into diamond through electronic excited states. *J. Phys. Condens. Matter.* 2003. V. 15. N 24. P. R1077.

61. **Meguro T., Hida A., Suzuki M., Koguchi Y., Takai H., Yamamoto Y., Maeda K., Aoyagi Y.** Creation of nanodiamonds by single impacts of highly charged ions upon graphite. *Appl. Phys. Lett.* 2001. V. 79. N 23. P. 3866-3868.

62. **Raman R.K., Murooka Y., Ruan C.-Y., Yang T., Berber S., Tománek D.** Direct Observation of Optically Induced Transient Structures in Graphite Using Ultrafast Electron Crystallography. *Phys. Rev. Lett.* 2008. V. 101. N 7. P. 077401.

63. **Scandolo S., Bernasconi M., Chiarotti G.L., Focher P., Tosatti E.** Pressure-Induced Transformation Path of Graphite to Diamond. *Phys. Rev. Lett.* 1995. V. 74. N 20. P. 4015-4018.

64. **Kampfrath T., Perfetti L., Schapper F., Frischkorn C., Wolf M.** Strongly Coupled Optical Phonons in the Ultrafast Dynamics of the Electronic Energy and Current Relaxation in Graphite. *Phys. Rev. Lett.* 2005. V. 95. N 18. P. 187403. DOI: 10.1103/PhysRevLett.95.187403.

65. **Mao W.L., Mao H.-K., Eng P.J., Trainor T.P., Newville M., Kao C.-C., Heinz D.L., Shu J., Meng Y., Hemley R.J.** Bonding Changes in Compressed Superhard Graphite. *Science.* 2003. V. 302. N 5644. P. 425-427.

66. **Chen S., Seidel M.T., Zewail A.H.** Atomic-scale dynamical structures of fatty acid bilayers observed by ultrafast electron crystallography. *PNAS.* 2005. V. 102. N 25. P. 8854-8859. DOI: 10.1073/pnas.0504022102.

67. **Ruan C.-Y., Yang D.-S., Zewail A.H.** Structures and Dynamics of Self-Assembled Surface Monolayers Observed by Ultrafast Electron Crystallography. *J. Am. Chem. Soc.* 2004. V. 126. N 40. P. 12797-12799.

68. **Китайгородский А.И.** Молекулярные кристаллы. М.: Наука. 1971. 424 с.

69. **Zanchet D., Tolentino H., Martins Alves M.C., Alves O.L., Ugarte D.** Inter-atomic distance contraction in thiol-passivated gold nanoparticles. *Chem. Phys. Lett.* 2000. V. 323. N 1–2. P. 167-172. DOI: 10.1016/S0009-2614(00)00424-3.

70. **Gao M., Lu C., Jean-Ruel H., Liu L.C., Marx A., Onda K., Koshihara S.-Y., Nakano Y., Shao X., Hiramatsu T., Saito G., Yamochi H., Cooney R.R., Moriena G., Sciaini G., Miller R.J.D.** Mapping molecular motions leading to charge delocalization with ultrabright electrons. *Nature.* 2013. V. 496. N 7445. P. 343-346. DOI: 10.1038/nature12044.

71. **Dwayne Miller R.J.** Ultrafast imaging of photochemical dynamics: roadmap to a new conceptual basis for chemistry. *Farad. Discuss.* 2016. V. 194. P. 777-828. DOI: 10.1039/C6FD00241B.

57. **Sundaram S.K., Mazur E.** Inducing and probing non-thermal transitions in semiconductors using femtosecond laser pulses. *Nat Mater.* 2002. V. 1. N 4. P. 217-224. DOI: 10.1038/nmat767.

58. **Fahy S., Louie S.G., Cohen M.L.** Pseudopotential total-energy study of the transition from rhombohedral graphite to diamond. *Phys. Rev. B.* 1986. V. 34. N 2. P. 1191-1199. DOI: 10.1103/PhysRevB.34.1191.

59. **Yang G.W., Wang J.B.** Pulsed-laser-induced transformation path of graphite to diamond via an intermediate rhombohedral graphite. *Appl. Phys. A.* 2001. V. 72. N 4. P. 475-479. DOI: 10.1007/s003390000537.

60. **Nakayama H., Katayama-Yoshida H.** Direct conversion of graphite into diamond through electronic excited states. *J. Phys. Condens. Matter.* 2003. V. 15. N 24. P. R1077. DOI: 10.1088/0953-8984/15/24/202.

61. **Meguro T., Hida A., Suzuki M., Koguchi Y., Takai H., Yamamoto Y., Maeda K., Aoyagi Y.** Creation of nanodiamonds by single impacts of highly charged ions upon graphite. *Appl. Phys. Lett.* 2001. V. 79. N 23. P. 3866-3868. DOI: 10.1063/1.1424047.

62. **Raman R.K., Murooka Y., Ruan C.-Y., Yang T., Berber S., Tománek D.** Direct Observation of Optically Induced Transient Structures in Graphite Using Ultrafast Electron Crystallography. *Phys. Rev. Lett.* 2008. V. 101. N 7. P. 077401. DOI: 10.1103/PhysRevLett.101.077401.

63. **Scandolo S., Bernasconi M., Chiarotti G.L., Focher P., Tosatti E.** Pressure-Induced Transformation Path of Graphite to Diamond. *Phys. Rev. Lett.* 1995. V. 74. N 20. P. 4015-4018. DOI: 10.1103/PhysRevLett.74.4015.

64. **Kampfrath T., Perfetti L., Schapper F., Frischkorn C., Wolf M.** Strongly Coupled Optical Phonons in the Ultrafast Dynamics of the Electronic Energy and Current Relaxation in Graphite. *Phys. Rev. Lett.* 2005. V. 95. N 18. P. 187403. DOI: 10.1103/PhysRevLett.95.187403.

65. **Mao W.L., Mao H.-K., Eng P.J., Trainor T.P., Newville M., Kao C.-C., Heinz D.L., Shu J., Meng Y., Hemley R.J.** Bonding Changes in Compressed Superhard Graphite. *Science.* 2003. V. 302. N 5644. P. 425-427. DOI: 10.1126/science.1089713.

66. **Chen S., Seidel M.T., Zewail A.H.** Atomic-scale dynamical structures of fatty acid bilayers observed by ultrafast electron crystallography. *PNAS.* 2005. V. 102. N 25. P. 8854-8859. DOI: 10.1073/pnas.0504022102.

67. **Ruan C.-Y., Yang D.-S., Zewail A.H.** Structures and Dynamics of Self-Assembled Surface Monolayers Observed by Ultrafast Electron Crystallography. *J. Am. Chem. Soc.* 2004. V. 126. N 40. P. 12797-12799. DOI: 10.1021/ja045441n.

68. **Kitaygorodsky A. I.** Molecular crystals. Nauka. 1971. 424 p. (in Russian).

69. **Zanchet D., Tolentino H., Martins Alves M.C., Alves O.L., Ugarte D.** Inter-atomic distance contraction in thiol-passivated gold nanoparticles. *Chem. Phys. Lett.* 2000. V. 323. N 1–2. P. 167-172. DOI: 10.1016/S0009-2614(00)00424-3.

70. **Gao M., Lu C., Jean-Ruel H., Liu L.C., Marx A., Onda K., Koshihara S.-Y., Nakano Y., Shao X., Hiramatsu T., Saito G., Yamochi H., Cooney R. R., Moriena G., Sciaini G., Miller R.J.D.** Mapping molecular motions leading to charge delocalization with ultrabright electrons. *Nature.* 2013. V. 496. N 7445. P. 343-346. DOI: 10.1038/nature12044.

71. **Dwayne Miller R.J.** Ultrafast imaging of photochemical dynamics: roadmap to a new conceptual basis for chemistry. *Farad. Discuss.* 2016. V. 194. P. 777-828. DOI: 10.1039/C6FD00241B.

20

Изв. вузов. Химия и хим. технология. 2017. Т. 60. Вып. 5